

Experimental assessment of slamming coefficients for subsea equipment installations

Allan C de Oliveira^{*} and Rafael G Pestana^a

Petrobras R&D Center, Petrobras, Av Horacio de Macedo, 950, Cidade Universitaria, Brazil

(Received December 11, 2019, Revised April 28, 2020, Accepted May 8, 2020)

Abstract. Considering the huge demand of several types of subsea equipment, as Christmas Trees, PLEMs (Pipeline End Manifolds), PLETs (Pipeline End Terminations) and manifolds for instance, a critical phase is its installation, especially when the equipment goes down through the water, crossing the splash zone. In this phase, the equipment is subject to slamming loads, which can induce impulsive loads in the installation wires and lead to their rupture. Slamming loads assessment formulation can be found in many references, like the Recommended Practice RP-N103 from DNV-GL (2011), a useful guide to evaluate installation loads. Regarding to the slamming loads, RP-N103 adopt some simplifying assumptions, as considering small dimensions for the equipment in relation to wave length, in order to estimate the slamming coefficient C_s used in load estimation. In this article, an experimental investigation based on typical subsea structure dimensions was performed to assess the slamming coefficient evaluation, considering a more specific scenario in terms of application, and some reduction of the slamming coefficient is achieved for higher velocities, with positive impact on operability.

Keywords: slamming; subsea engineering; model testing; subsea equipment installation

1. Introduction

Deep and ultra-deep water oil production has been demanding a huge quantity of different types of subsea equipment, as Xmas Trees, PLETs, PLEMs, manifolds and so on. There is also some technological push to transfer some parts of oil processing facilities, like primary separation (Kuchpil *et al.* 2013) or gas separation, to subsea (Albuquerque *et al.* 2013), decreasing the size of the production platform. Fig. 1 shows a manifold crossing the splashing zone during its installation.

A critical step during installation is the equipment entry through the sea surface due to slamming loads, which may cause slacking of the installation wires, increasing the risk of the operation. Slamming loads are estimated according to the Recommendation Practice RP-N103 from DNV-GL (2011), which presents some simplifying assumptions to evaluate the slamming coefficient C_s . For instance, a first assumption considers the entire bottom area of the structure hit simultaneously by the wave. It is also not usual to consider the porosity of the bottom structure, as

^{*}Corresponding author, D.Sc., E-mail: allan_carre@petrobras.com.br

^a M.Sc., E-mail: rafaelpestana@petrobras.com.br



Fig. 1 Subsea manifold crossing the splash zone, courtesy from Petrobras

shown in manifold in Fig. 1, on slamming load computations.

Aiming to improve the comprehension of these effects and increase the availability of safe operational conditions in which to perform these operations, an extensive model test campaign was performed in the Numerical Offshore Tank (TPN) facilities in São Paulo University, and C_S values were obtained for several different test configurations, as is shown along in the present work.

2. Slamming coefficient

Slamming loads are an almost centenary subject topic of studies. First references came from Von Karman (1929) and Wagner (1931, 1932) studies for seaplanes. For Naval Architecture purposes, slamming loads are also important for ship and high-speed vessel load evaluations, and references like Verhagen (1967), Hagiwara *et al.* (1976) and Koehler *et al.* (1977) have stressed the influence of the angle between the edge and the sea surface on slamming load values.

Slamming impact evaluations are common for ships (Dhavalikar *et al.* 2018) offshore structures and recently for wind farm offshore foundations (Paulsen *et al.* 2019) and are also relevant during subsea equipment installation operations when it is crossing the splashing zone. This phenomenon is strongly nonlinear, including effects such as flow separation and jet flows that are usually hard to model numerically, although there are references that evaluates slamming coefficients using Computational Fluid Dynamics (CFD) (Seif *et al.* 2005).

Regarding subsea equipment slamming during its installation, loads are usually evaluated according to DNV Recommendation Practices RP-N103 (2011). Although this reference allows and discuss how slamming assessments should be made, it also proposes a simplified method, which is widely used by the industry and is considered in the comparisons made in this article. The recommendation also uses as reference model tests performed at Marintek, by Øritsland (1989).

Traditional slamming approach involves analytical model and experiments, as shown by Newman (1977) and Faltinsen (1990). Considering an infinite cylinder (2D problem), potential

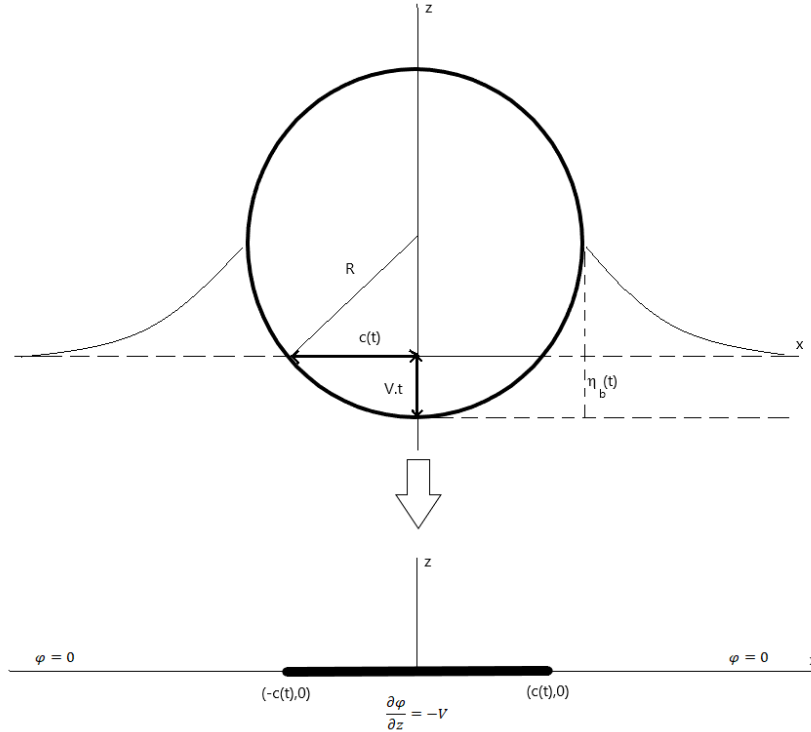


Fig. 2 Simplified approach to the slamming problem

theory (incompressible and irrotational flow) and that the cylinder represented by a flat plate of chord $2 \cdot c(t)$ while entering the water, a simplified approach to the slamming problem is shown in Fig. 2.

By potential theory

$$\nabla^2 \varphi = 0, \quad \text{in the fluid domain} \quad (1)$$

$$\varphi = 0, \quad \text{at the free surface} \quad (2)$$

$$\frac{\partial \varphi}{\partial z} = -V, \quad \text{at } Z=0 \quad (3)$$

$$\frac{\partial \varphi}{\partial n} = n_1 \frac{\partial \varphi}{\partial x} + n_3 \frac{\partial \varphi}{\partial z} = -V n_3 \quad \text{at "flat plate"} \quad (4)$$

According to Newman (1977) and Faltinsen (1990), the potential function φ can be written as

$$\varphi = -V(c(t)^2 - x^2)^{\frac{1}{2}}, \quad \text{for } -c(t) < x < c(t) \quad (5)$$

Using Bernoulli's equation to evaluate pressure

$$p = -\rho \frac{\partial \varphi}{\partial t} - \rho g z - \frac{\rho}{2} \left(\left(\frac{\partial \varphi}{\partial x} \right)^2 + \left(\frac{\partial \varphi}{\partial z} \right)^2 \right) + C \quad (6)$$

At $z = 0$, $\rho g z = 0$. The constant C also can be eliminated by using atmospheric pressure as reference. Finally, V^2 is usually $\ll \rho \partial \varphi / \partial t$, leading to the following pressure formulation

$$p = -\rho \frac{\partial \varphi}{\partial t} = \rho V \frac{c(t)}{(c(t)^2 - x^2)^{\frac{1}{2}}} \frac{dc}{dt} \quad (7)$$

And the force by length formulation becomes

$$F = \int_{-c(t)}^{c(t)} p \cdot dx = \rho V c(t) \frac{d}{dt} \int_{-c(t)}^{c(t)} \frac{1}{[c(t)^2 - x^2]^{\frac{1}{2}}} dx = V \frac{d}{dt} \left[\rho \frac{\pi}{2} c(t)^2 \right] \quad (8)$$

Replacing $c(t)$ as

$$\begin{aligned} R^2 &= c(t)^2 + (R - Vt)^2 \\ R^2 &= c(t)^2 + R^2 - 2VtR + V^2t^2 \\ c(t)^2 &= 2VtR - V^2t^2 \end{aligned} \quad (9)$$

Which leads to

$$F = \rho V \frac{\pi}{2} \frac{d}{dt} (2VtR - V^2t^2) = \rho V \frac{\pi}{2} (2VR - 2tV^2) \quad (10)$$

At $t = 0$ (first impact) and replacing $D = 2R$, the force per unit length becomes

$$F = \rho V \frac{\pi}{2} (2VR) = \pi \frac{\rho V^2}{2} D \quad (11)$$

And the force acting on the cylinder if length L becomes

$$F_S = \pi \frac{\rho V^2}{2} DL \quad (12)$$

Similar to hydrodynamic drag, the slamming force according to this approach becomes proportional to the square of the impact velocity. The slamming coefficient C_S can thus be defined as

$$C_S = \frac{F_S}{\frac{1}{2} \rho V^2 A} \quad (13)$$

Subsea equipment slamming load evaluation follows a similar path, according to DNV-RP-N103 (2011). This reference cites another Recommendation Practice, the DNVGL-RP-C205 (2010), sections 3.2.9 (Slamming Force) and 3.4.2 (Regular Design Wave Approach), where the slamming force is computed using the following formulation in still waters

$$F_S(t) = \frac{d(A_{33}^{\infty} v_S)}{dt} = v_S \frac{d(A_{33}^{\infty})}{dt} = \frac{1}{2} \rho C_S A_S v_S^2 \quad (14)$$

Where $A_{33}^{\infty}(t)$ is the added mass computed in infinite frequency for the instantaneous geometry at each time t , using a Boundary Element Method (BEM) software like WAMIT, C_S is the slamming coefficient, A_S is the projected area of the object and V_S is the impact speed. In waves, the speed needs to be corrected by the wave amplitude velocity in the vertical direction, v , as shown below

$$F_S = \frac{1}{2} \rho C_S A_S (v - \dot{\eta})^2 \quad (15)$$

Where ρ is the seawater specific mass, C_S is the slamming coefficient, A_S is slamming projected area into the horizontal plane, v is the wave particle vertical velocity at A_S and $\dot{\eta}$ is the object vertical velocity. The slamming coefficient can be determined by numerical or experimental techniques. For cylinders, it should not be less than 3.0. For other shapes, it should be less than 5.0, according to DNV-RP-C205 (2010).



Fig. 3 Wave Basin at the Numerical Offshore Tank, University of São Paulo

3. Model tests

As mentioned by DNV Recommendation Practices RP-N103 (2011) and RP-C205 (2010), slamming coefficients can be determined by experimental evaluations. The experimental assessment was performed at the wave basin of the Numerical Offshore Tank (TPN – Tanque de Provas Numérico) at São Paulo University (Fig. 3). The wave basin has 14 m of length and breadth, and 4 meters of depth. The tests were done using a scaling factor of 1:35, as shown in Table 1 (Mello and Malta 2018).

Table 1 Scaled models dimensions

	Prot. (m)		3		6		9.5		12			
Length	Prot. (m)	3		6		9.5		12				
	Model (mm)	85.7		171.4		271.4		342.9				
Breadth	Prot. (m)	3.0		3.0		3.0		3.0				
	Model (mm)	85.7		85.7		85.7		85.7				
Porosity (%)	0	5	15	0	5	15	0	5	15	0	5	15
Holes	Diam. (mm)	5.5	5.5	5.5	5.5	5.5	5.5	5.5	5.5	5.5	5.5	5.5
	#	16	49	32	98	48	154	64	196	64	196	196
	# x #	4x4	7x7	4x8	7x14	4x12	7x22	4x16	7x28	4x16	7x28	7x28
Measured Porosity(%)	5.17	15.85	15.85	5.17	15.85	15.85	4.90	15.73	15.73	5.17	15.85	15.85
Model ID	M01	M02	M03	M04	M05	M06	M07	M08	M09	M10	M11	M12

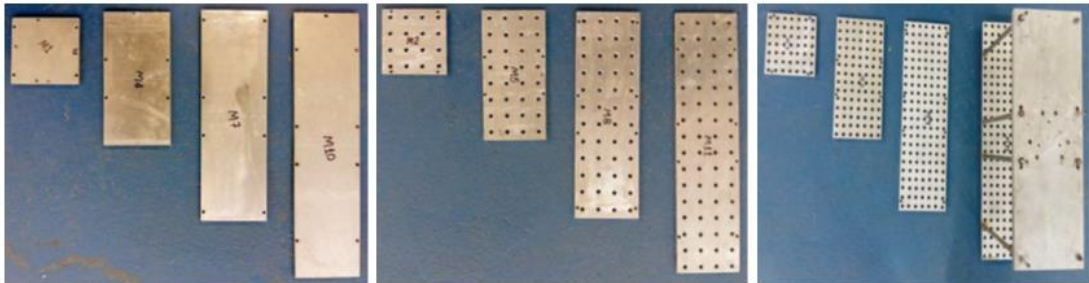


Fig. 4 Simplified models for slamming test

Table 2 Manifold model dimensions

	M13 (with mudmat)		M14 (without mudmat)	
	Prototype	Model	Prototype	Model
Length	15.5 m	442.9 mm	15.5 m	442.9 mm
Breadth	9.5 m	271.4 mm	8.4 m	240.0 mm
Height	6.8 m	194.3 mm	6.8 m	194.3 mm
Weight	190 ton	4.431 kg	190 ton	4.431 kg

Table 3 Still water tests impact velocities

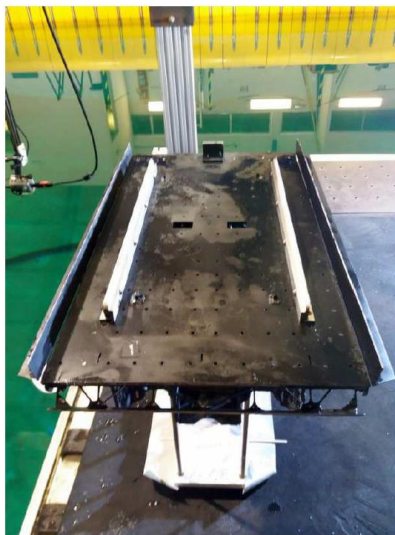
Velocity	Model Scale	Prototype Scale
V01	33 mm/s	0.195 m/s
V02	101 mm/s	0.597 m/s
V03	169 mm/s	1.000 m/s
V04	236 mm/s	1.396 m/s
V05	301 mm/s	1.780 m/s

The models represent the bottom geometry (mudmat) of the subsea equipment and consist of aluminium plates. These plates are thick enough to suffer negligible deformations due to the impact loads during the tests. The plates have the same breadth but four different lengths, in order to evaluate running wave effects on the slamming coefficient results. The plates also present different levels of porosity (0%, 5% and 15% of the area) in order to evaluate their effect on the results. It totalizes 12 different configurations of simplified models, as shown in Fig. 4 and Table 1.

Besides the simplified plate models, a manifold model [10] was also tested in two different configurations: with its mudmat and without its mudmat, as shown in Fig. 5 and Table 2.



(a)



(b)



(c)

Fig. 5 Subsea manifold model (scale 1:35). (a) Top view, mudmat configuration; (b) bottom view, mudmat configuration (M13); (c) bottom view, w/o mudmat configuration (M14)

The tests were performed considering three different load categories: still water, with impact velocity controlled by an actuator; fixed model under the action of regular waves and fixed model under the action of irregular waves. The still water tests were carried out considering five different impact velocities, as shown in Table 3.

The regular wave tests were carried out considering 30 impact cycles for slamming force evaluation, while the irregular waves consider 1826 seconds, representing 10800 seconds in the prototype scale. Considering regular and irregular waves, 13 different waves in a total of 252 different tests were considered, comprising all configurations. Tables 4 and 5 show the regular and irregular waves tested.

Table 4 Regular waves tested

Wave	Type	Height (H)/Amplitude (A)		Peak Period (s)		$V = \omega A$
		Model (H)	Prototype (A)	Model	Prototype	
W004	Regular	87.54 mm	1.53195 m	1.01	5.97516	1.6109 m/s
W005	Regular	84.47 mm	1.4782 m	1.35	7.9866	1.1629 m/s
W006	Regular	85.79 mm	1.5013 m	1.7	10.0572	0.9379 m/s
W007	Regular	86.34 mm	1.511 m	2.04	12.0686	0.7866 m/s
W008	Regular	82.55 mm	1.4446 m	2.35	14.4942	0.6262 m/s
W009	Regular	115.94 mm	2.02895 m	1.01	5.97516	2.1325 m/s
W010	Regular	113.69 mm	1.98958 m	1.35	7.9866	1.5644 m/s
W011	Regular	114.93 mm	2.01128 m	1.7	10.0572	1.2559 m/s
W012	Regular	114.58 mm	2.00515 m	2.04	12.0686	1.0434 m/s
W013	Regular	110.23 mm	1.92903 m	2.35	14.4942	0.8357 m/s

Table 5 Irregular waves tested

Wave	Type	H_s (m)	T_p (s)	V_{MAX} (m/s)
W001	Irregular	1.99	8.08	1.955
W002	Irregular	2.00	10.10	1.759
W003	Irregular	2.01	11.54	1.656

For the irregular waves, the maximum velocity was estimated considering the wave spectra, according to the following relation

$$V_{max} \approx 4.0 \sqrt{\int_0^{\infty} \omega S(\omega) d\omega} \quad (16)$$

The slamming coefficient corrected due to porosity C_{SP} is defined as

$$C_{SP} = \frac{Fz}{0.5\rho(A)V^2} \quad (17)$$

Where A is the real area of the plate (discounting porosity) or $LB(1-p)$ where L is the plate length, B is the plate breadth and p is the porosity (0, 0.05 or 0.15). For irregular waves, V_{max} is considered as velocity impact, replacing V in Eq. (17).

4. Results

Due to the amount of data, the results are presented in graph form. An important first assessment can be observed in Fig. 5, which shows the slamming coefficient in function of impact velocity. It can be noted a good agreement of the results with the trend line (represented by the correlation factor R and obtained considering all tested situations: still water, regular waves and irregular waves) and a negligible influence of the periodicity of the waves on results.

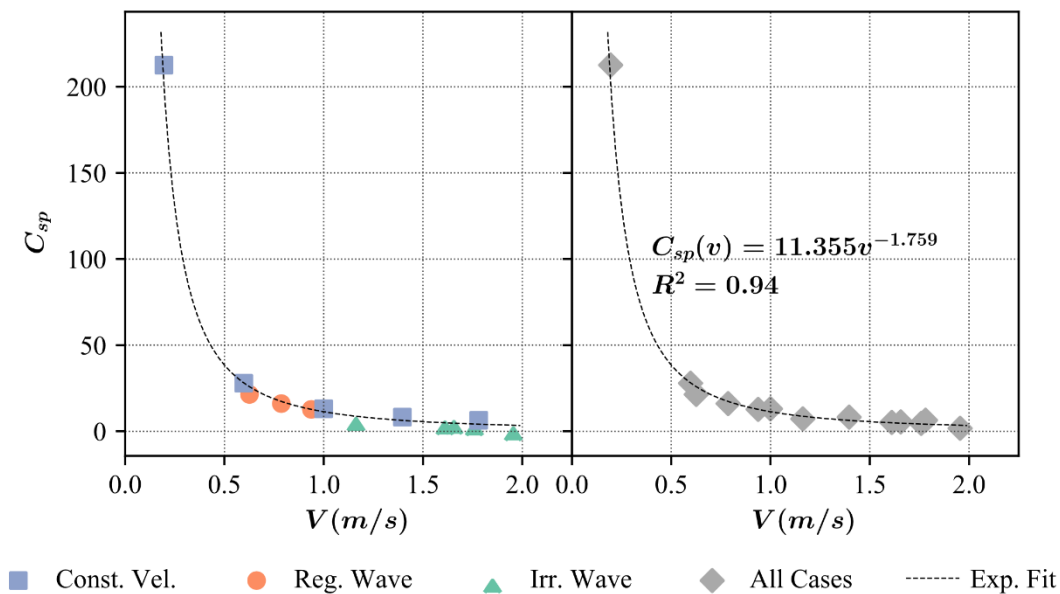


Fig. 6 C_{SP} in function of impact velocity for model M01

The right side of Fig. 6 shows the behavior of the C_{SP} coefficient in function of the impact velocity grouping the results of impacts in still water, regular and irregular waves, used to obtain the trend line exponential fit. Although these references do not treat subsea equipment slamming, they have already shown that flat bottom (0 degree of dead rise angle) presents greater values for slamming coefficients. Considering a very small velocity, where the potential velocity approximation becomes more accurate, the results presented in the article are more consistent with Wagner (1931, 1932) theory results, asymptotically for flat bottom.

The behavior shown in Fig. 6 repeats itself for all plate results. Fig. 7 shows separate plate results in the left-hand graph in order to verify how plate length and porosity affects the overall results. Considering the area correction for porosity, neither porosity or length has a significant influence in the results, or, as shown in right-hand side of Fig. 7, the grouped plates results fit can also be considered for C_{SP} estimation with reasonable accuracy.

The inclusion of the manifold results, however, introduces significant differences in the slamming results, as shown in Fig. 8. One of the differences between the manifold and the plates is manifold breadth, which is considerably larger than the plates. In order to verify its influence and present the results in a non-dimensional form, a non-dimensional parameter to represent velocity becomes necessary.

There are several ways to rewrite some model parameters in non-dimensional form. A very common way to do this is applying Buckingham Pi's Theorem (Chakrabarti 1994). In the present work, however, a search in literature for common parameters to represent impact velocity in slamming

was performed. Santos (2013) and Pesce *et al.* (2006) use Froude's number to make the velocity non-dimensional. Froude's number, considering Naval Architecture standards (Lewis 1988), usually considers length to build the non-dimensional relation. However, since it was observed that the length was not relevant to the slamming coefficient evaluation and that breadth seems to play an important role in the slamming coefficient behavior, it was chosen to compose the Froude Number to be used, according to the following definition

$$Fr = \frac{v}{\sqrt{gB}} \quad (18)$$

Where B is the breadth (perpendicular to the wave propagation direction) of the element subject to slamming effects, as shown in Fig. 9.

Adjusting the data of the graph in Fig. 8 to the Froude number defined in Eq. (18) results in better agreement between plate and manifold results, as shown in Fig. 10. The insert graph shows a more detailed view into the higher Froude number range, more critical for subsea installations, and it can be noted that the fit generated for the plates represents the manifold behavior slightly conservatively in most of the cases, and it was adopted due to the better correlation factor achieved.

Because the highest Froude number tested is 0.36, for greater values the slamming coefficient was kept constant. In that way, the slamming coefficient formulation becomes

$$\begin{cases} C_s = 0.601082Fr^{-1.738831} , Fr < 0.36 \\ C_s = 3.551082 , Fr \geq 0.36 \end{cases} \quad (19)$$

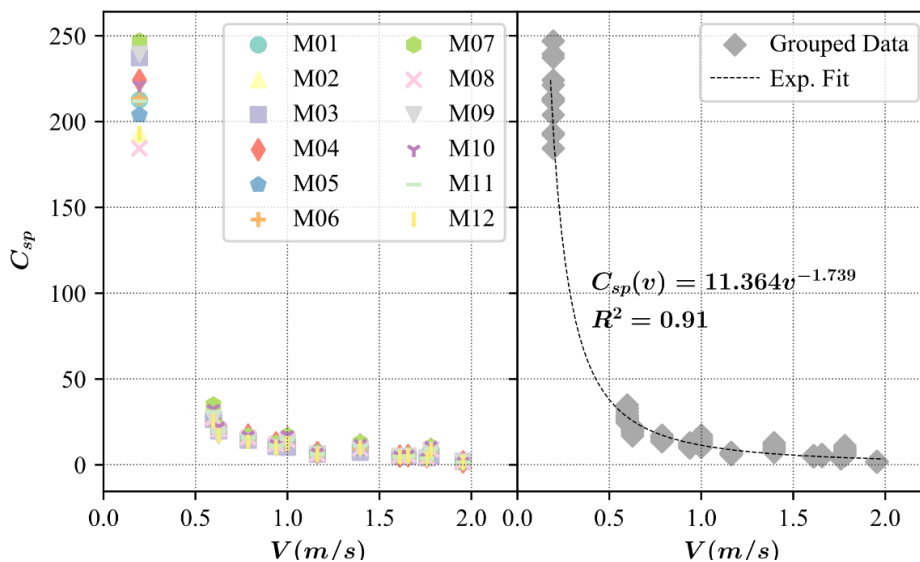


Fig. 7 C_{SP} in function of impact velocity for all plate models

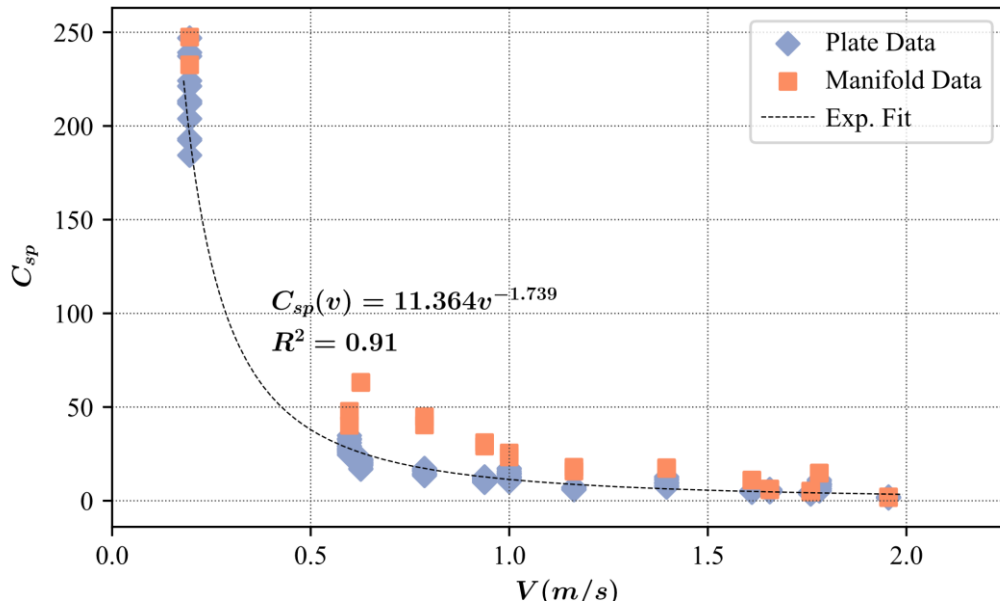


Fig. 8 C_{SP} in function of impact velocity for all plate models and manifold

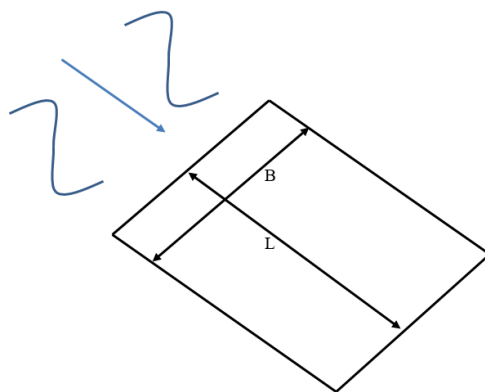


Fig. 9 Object breadth and length definition in relation to wave propagation direction

Which are the implications of using this formulation, instead of DN-RP-N103 recommendations? Fig. 11 shows a comparison at same basis for both formulations and it can be noted that this formulation reduces the slamming coefficients for Froude numbers above 0.3.

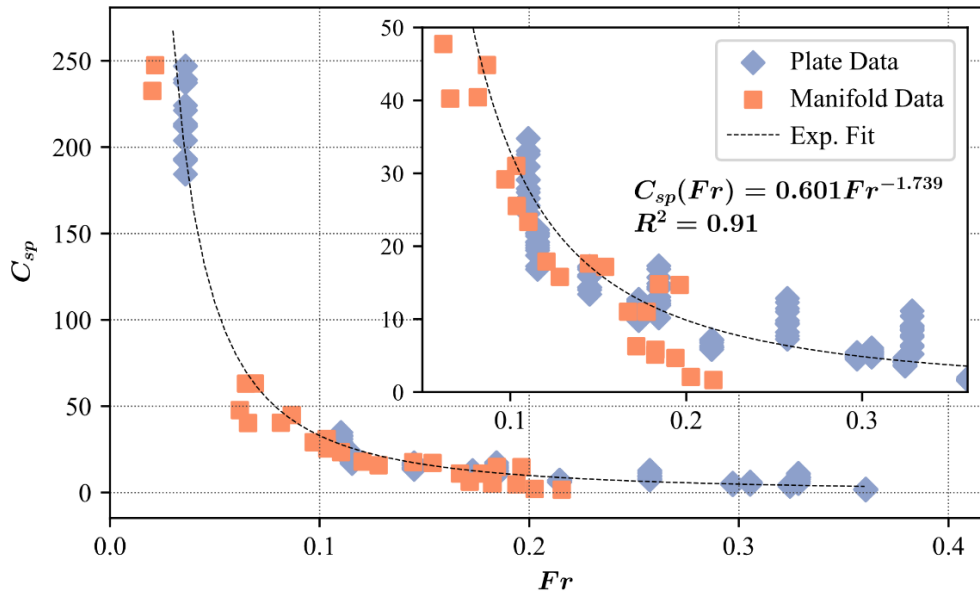


Fig. 10 C_{sp} in function of Froude number for all plate models and manifold

In order to understand the impact of the change of formulation, a hypothetical manifold installation operation was analyzed through a sensitivity study. According to the Recommended Practice DNV-RP-N103, a simplified expression may be utilized to estimate the slamming impact velocity, as shown below

$$V_s = V_c + \sqrt{V_w^2 + V_{ct}^2} \quad (20)$$

Where V_s is slamming impact velocity, V_c is the wire lowering velocity, V_w is the characteristic vertical wave particle velocity and V_{ct} is the characteristic vertical vessel crane tip velocity. Irregular waves were assumed, following the JONSWAP spectrum, and single amplitude most probable maximum values during a 3-hour realization were considered to calculate V_w . A typical installation vessel RAO (Response Amplitude Operator) was assumed to estimate V_{ct} , also based on single amplitude most probable maximum value in 3 hours. V_c was assumed as 0.5 m/s.

For this hypothetical study, a manifold of different dimensions compared to the tested (see Table 6) was assessed. For different sea states, the slamming coefficients were evaluated according to Eq. (19) and the results are presented in Table 7. It can be noted that this formulation reduces slamming loads for shorter period waves, which is an expected result and has potential to extend the safe conditions for subsea equipment installation operations during lowering through the splash zone.

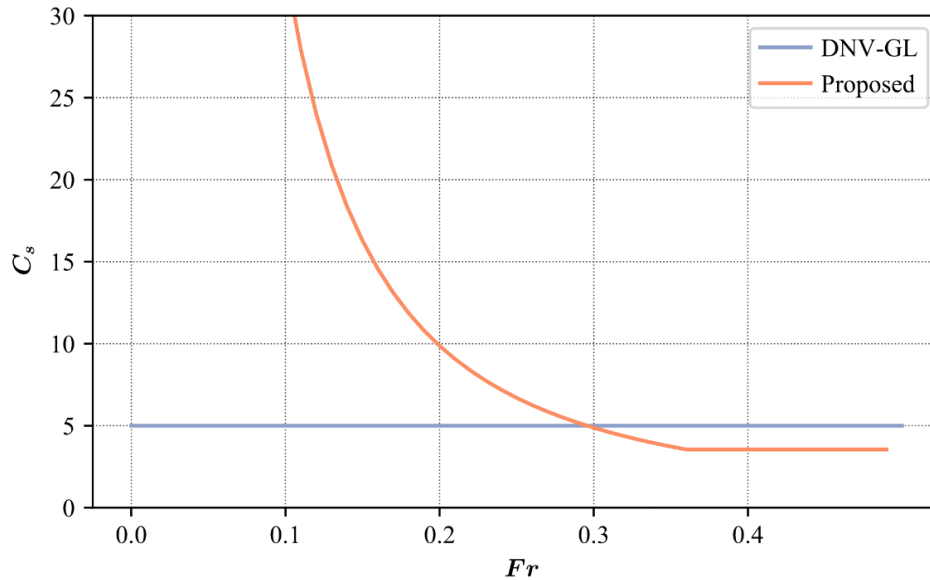


Fig. 11 Comparison between DNV-RP-N103 and proposed formulation

Table 6 Sensitivity study manifold dimensions

Equipment	Dimension
Mudmat breadth	10.14 m
Mudmat length	15.46 m

The bold italic values on Table 7 shows the sea states that would use slamming coefficients greater than DNV references. Shorter periods, usually less than 8 seconds, are typically more critical to slamming load evaluations, due to higher wave particle velocity. The proposed formulation leads to reduced slamming loads for these cases.

Eq. (19) also brings an important concern about slamming loads for smaller velocities, when the Froude number is less than 0.2. As shown in Fig. 11, for that region, the slamming coefficients are greater than those specified by DNV-RP-N103. To better understand what happens to slamming forces, a graphical plot of the evolution of the slamming coefficient and slamming pressure in relation to velocity is shown for the same manifold dimensions described in table 6 (Fig. 12). It can be noted that, despite the fact that the slamming coefficient decreases with increasing velocity (and, consequently, Froude number), the slamming pressure itself still increases. It means that, observing Table 7, the highest slamming pressure values are associated with the smallest slamming coefficients, and, if Table 7 was computed considering DNV-RP-N103 simplification, greater values of slamming pressure would be obtained, being conservative in this case, in relation to the proposed formulation.

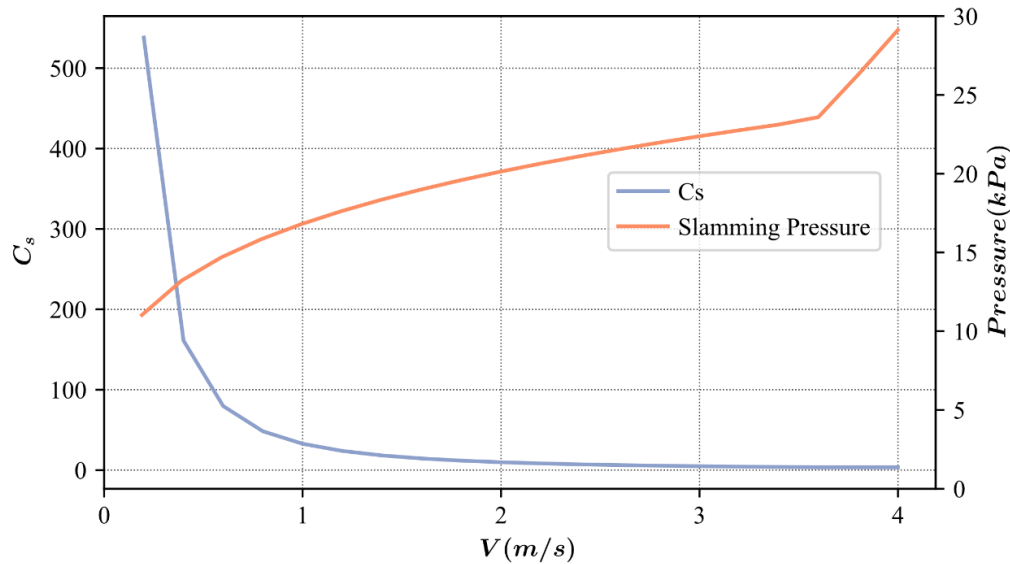


Fig. 12 Comparison between slamming pressure and slamming coefficient considering the proposed formulation

The behavior observed in this verification is quite like what is seen in other slamming assessments performed internally in the past (Oliveira 2015, Pestana 2014), where the critical region for slamming was at the same period and H_s combinations region. It leads to a perception that critical slamming loads for such type of structure usually occurs for velocities over the $Fr > 0.2$ limit, where the proposed formulation for slamming force leads to lower values than the one recommended by DNV RP-N103. It is important to remark that this observation does not exclude the possibility of a particular equipment presenting greater values of slamming force computed by the proposed formulation.

5. Conclusions

This article proposes an alternative slamming coefficient formulation, based on experiments of representative dimensions of typical subsea equipment used in offshore oil and gas fields development. The tests were performed at São Paulo, in the TPN wave basin. About 252 tests were carried out, varying base dimensions and porosities.

As results, the plate's tests showed good correlation between slamming impact force and velocity. Wave declination effects could be neglected, since the results followed the same trend shown in still water tests, and grouped data (waves and still water tests) results also presented a good correlation.

Table 7 Sensitivity study C_{SP} results

T_P (s)	H_s (m)			
	1.5	2.0	2.5	3.0
4.0	4.09	3.55	3.55	3.55
4.5	4.86	3.55	3.55	3.55
5.0	5.65	3.72	3.55	3.55
5.5	6.46	4.27	3.55	3.55
6.0	7.26	4.84	3.55	3.55
6.5	8.05	5.39	3.89	3.55
7.0	8.83	5.95	4.31	3.55
7.5	9.62	6.52	4.74	3.63
8.0	10.40	7.08	5.17	3.96
8.5	11.01	7.53	5.51	4.23
9.0	11.53	7.91	5.81	4.46
9.5	11.98	8.24	6.06	4.67
10.0	12.34	8.51	6.27	4.83
10.5	12.56	8.67	6.39	4.93
11.0	12.70	8.78	6.47	5.00
11.5	12.93	8.95	6.61	5.10
12.0	13.33	9.25	6.84	5.29
12.5	13.86	9.65	7.15	5.54
13.0	14.43	10.08	7.48	5.80
13.5	14.99	10.50	7.82	6.07
14.0	15.53	10.91	8.14	6.34

Manifold tests were slightly more dispersed. However, considering the non-dimensional form adopted (impact velocity represented by Froude number), a good description of manifold slamming behavior could be achieved using plate slamming coefficient formulation.

The sensitivity study performed showed that the use of the proposed slamming formulation reduces slamming loads in the usual most critical cases for slamming assessment, like shorter wave periods with higher wave heights, in comparison with DNV-RP-N103 prescribed coefficient. On the other hand, for longer wave periods the formulation leads to higher slamming load estimates, although, in typical subsea equipment installation scenarios, the formulation would likely result in expanded safe operational conditions.

6. Future work

Some aspects of the test results deserve further investigation. The manifold results dispersion is one of these aspects. Both manifold topology and mudmat topology may have introduced the

spreading observed in the results. To understand the importance of each aspect, an extra campaign should be performed in order to improve its understanding.

Another behavior that is expected but not observed was some difference between still water and wave tests due to wave declination effect on impact area. Wave parameters and equipment dimensions were based in the range of the most common subsea equipment installation operations performed by the industry. Because of that, the ratio between wave and equipment length has varied from 100 times (longest) to 5 times (shortest). Even the shortest ratio may be high enough mask wave declination effects, so that shorter ratios would be needed to make this effect evident on slamming results. This can be investigated in another test campaign.

Acknowledgments

The authors would like to thank the Petrobras R&D Center for the financial support, especially Mr. Daniel Fonseca de Carvalho e Silva who made available the wave basin tests presented in this article. The TPN team responsible for the tests is also acknowledged, specially Mr. Edgard Borges Malta and Mr. Pedro Cardozo de Mello.

References

- Albuquerque, F.A., Vianna, F.L.V., Alves, R.P., Kuchpil, C., Morais, M.G.G., Orłowski, R.T.C. and Ribeiro, O. (2013), "Subsea processing systems: Future vision", *Proceedings of the Offshore Technology Conference*, Houston, May. [https://doi:10.4043/24161-MS](https://doi.org/10.4043/24161-MS).
- Chakrabarti, S.K. (1994), *Offshore Structure Modeling*, Advanced Series on Ocean Engineering, Vol. 9, World Scientific, 1994.
- Chuang, S.L. (1966), "Slamming of Rigid Wedge-Shaped Bodies with Various Deadrise Angles", David Taylor Model Basin, Report 2268, Washington.
- Dhavalikar, S., Dabbi, P.N., Awasare, D.P., Poojari, D., Joga, R. and Kar, A.R. (2018), "Development of empirical formulations of slamming loads for displacement vessels", *Ocean Eng.*, **159**, 563-580.
- DNV-RP-C205 (2010), *Environmental Conditions and Environmental Loads*; Det Norske Veritas, Oslo, Norway.
- DNV-RP-N103 (2011), *Modelling and Analysis of Marine Operations*, Det Norske Veritas, Oslo, Norway.
- Faltinsen, O.M. (1990), *Sea Loads on Ships and Offshore Structures*, Cambridge University Press, Cambridge, United Kingdom.
- Hagiwara, K. and Yuhara, T. (1976), "Fundamental study of wave impact loads on ship bow", *J. Soc. Nav Arch., Japan*, **14**, 73-85.
- Koehler, B.R. and Kettleborough, C.F. (1977), "Hydrodynamic impact of a falling body upon a viscous incompressible fluid", *J. Ship Res.*, **21**(3), 165-181.
- Kuchpil, C., Duarte, D.G., Orłowski, R., Euphemio, M.L., Albuquerque, F.A. and Morais, M.G.G. (2013), "Subsea processing and boosting in Brazil: Status and future vision", *Proceedings of the Offshore Technology Conference*, Houston, May. [https://doi:10.4043/24498-MS](https://doi.org/10.4043/24498-MS)
- Lewis, Edward V. (1988), "Principles of Naval Architecture: Volume II: Resistance, Propulsion and Vibration", Society of Naval Architects and Marine Engineers (SNAME), Alexandria, VA, USA.
- Mello, P.C.M. and Malta, E.B.M (2018), "Relatório Final de Ensaio para Avaliação do Coeficiente de Slamming na Splashing Zone para Instalação de Módulos Submarinos", (Final Report for Slamming Coefficient Assessment over Splash Zone for Subsea Equipment Tests), Numerical Offshore Tank, São Paulo University (In Portuguese).

- MIT (2001), *WAMIT 6.0, A Radiation, Diffraction Panel Program for Wave Body Interactions*, Cambridge: The MIT Press, Cambridge, MA, USA.
- Newman, J.N. (1977), *Marine Hydrodynamics*, Cambridge: The MIT Press, Cambridge, MA, USA.
- Oliveira, A.C. (2015), “Análise de Instalação Pendular do Manifold de Albacora Leste” (Albacora Leste Manifold Installation Analysis Considering Pendulum Installation Method), CT TDUT 033/2015, Petrobras Internal Report.
- Øritsland, O. (1989), “A Summary of Subsea Module Hydrodynamic Data”, Marintek Report No.511110.05.
- Paulsen, B.T., Sonnevile, B., Meulen, M. and Jacobsen, N.G. (2019), “Probability of wave slamming and the magnitude of slamming loads on offshore wind turbine foundations”, *Coast. Eng.*, **143**, 76-95.
- Pesce, C.P., Tannuri, E.A. and Casetta, L. (2006), “The Lagrange equations for systems with mass varying explicitly with position: some applications for offshore engineering”, *J. Brazilian Soc. Mech. Sci. Eng.*, **28**(4), 496-504.
- Pestana, R.G. (2014), “Análise de Instalação a Cabo da BAP CCB-226 em Jubarte por Meio do RSV Far Saga” (BAP Analysis Installation fo Jubarte Field Using Far Saga Installation Vessel), CT TDUT 015/2014, Petrobras Internal Report.
- Santos, F.M (2013), “Impacto Hidrodinâmico Vertical de Corpos Axissimétricos Através de uma Abordagem Variacional” (Hydrodynamic Vertical Impact of Axissymmetrical Bodies Through a Variational Approach), Ph.D Dissertateation, Escola Politécnica da Universidade de São Paulo (Polytechnical School of Engineering os University of São Paulo), São Paulo, Brazil. (Doctoral Thesis in portuguese).
- Seif, S.M., Mousaviraad, S.M., Saddathosseini, S.H., Bertram, V. (2005), “Numerical modeling of 2-D water impact in one degree of freedom”, *Síntesis Tecnológica*, **2**(2), 79-83.
- Verhagen, J.H.G. (1967), “The impact of a flat plane on a water surface”, *J. Fluid Mech.*, **182**, 149-168.
- von Karman, T. (1929), “The impact of seaplane floats during landing”, NACA, Technical Note 321, Washington.
- Wagner, H. (1931), “Landing of Seaplanes”, Hampton, NACA/NASA Langlay Research Center, ,1931, Technical Memorandum n.622.
- Wagner, H. (1932), “Über Stoss und Gleitvorgänge an der Oberfläche von Flüssigkeiten. Zeitschr. F. Angewndte Mathematik und Mechanik, **12**(4), 193-235.